nature communications

Article

https://doi.org/10.1038/s41467-026-71122-7

# Pathways to cost-optimal and net-zero emissions irrigation in the United States

Received: 18 March 2025

Accepted: 13 March 2026

Published online: 27 March 2026

Check for updates

Jara Späte[1,2], Stefano Mingolla[1,3] & Lorenzo Rosa[1]

Irrigated agriculture enhances crop yields and climate resilience but also contributes to $CO_2$ emissions through energy use. Here, we apply energy system modeling to evaluate cost-emission trade-offs in electrified irrigation across the United States, integrating hourly energy production and historical water demand. We find that current practices are highly inefficient, leading to 23% (0.89 billion US dollar) higher costs and 39% (3.8 million metric tons of $CO_2$) more $CO_2$ emissions compared to the cost-optimal scenario, primarily due to reliance on diesel water pumps and limited solar photovoltaic adoption. Under cost-optimal conditions, 6.6 gigawatt of solar photovoltaic is deployed, and electric water pump installation capacity increase by 14% (11.3 $10^6$ $m^3h^{-1}$) relative to current levels. Emission reductions of 85% are achievable at marginal additional cost (+0.7%), whereas reaching net-zero roughly doubles system costs relative to business-as-usual. Renewable-powered electrified irrigation can thus deliver substantial, low-cost emission reductions but requires operational adaptation to solar-based systems.

Humanity faces the dual challenge of increasing food production to sustain a growing and wealthier population[1], while mitigating the environmental impacts of agriculture[2]. At the same time, global warming is expected to alter rainfall patterns and intensify the frequency and severity of droughts, although these changes will vary regionally and are subject to uncertainties in climate projections[3,4]. This is particularly concerning given that approximately 80% of global agricultural land relies on rain-fed systems, which are vulnerable to droughts[5,6].

Irrigated cropping systems offer a viable solution, providing higher yields than rain-fed agriculture and enhancing resilience by reducing dependence on unpredictable rainfall[7]. However, irrigation accounts for ~90% of global water consumption, making it a primary driver of global water scarcity[8], which leads to aquifers, rivers, lakes, and environmental flows depletion[9–11]. Moreover, as global temperatures rise, water availability for irrigation is becoming increasingly uncertain, amplifying risks to agricultural sustainability[12,13]. Additionally, irrigation itself contributes to greenhouse gas emissions, primarily through energy-intensive water pumping[14], emitting about 213 million metric tons of carbon dioxide (Mt $CO_2$) annually worldwide, or 0.6% of global $CO_2$ emissions[15]. Groundwater pumping accounts for 91% of these emissions, with diesel-powered pumps contributing 55% and electric pumps 45%, highlighting the potential for electrified low-carbon systems to reduce emissions[15,16]. In the United States (U.S.), energy-related emissions from irrigation were 12.6 Mt $CO_2$ in 2018, with emissions varying by energy source, crop type, and location[17]. Recent work has also quantified additional greenhouse gas emissions from nitrous oxide, groundwater degassing, and water transfers, underscoring the broader climate impacts of irrigation practices[18,19].

Efforts to reduce energy-related emissions from irrigation have highlighted promising solutions[15]. The introduction of energy- and water-efficient irrigation systems, such as low-energy precision application and drop nozzle spray systems, can cut energy use by ~20% and greenhouse gas emissions by ~15%[20]. These technologies use less water than traditional systems by minimizing evaporative losses, lowering flow rates, and reducing pressurization requirements[21]. Other studies have proposed using renewables to power electric water pumps to reduce $CO_2$ emissions from irrigation practices[15,17,21,22]. Agrivoltaics, the simultaneous use of land for agriculture and solar photovoltaic (PV) systems energy production, could offer benefits such as reducing plant drought stress, increasing crop yields, and improving solar PV panel energy efficiency[23].

[1]Biosphere Sciences and Engineering, Carnegie Institution for Science, Stanford, USA. [2]Department of Mechanical and Process Engineering, ETH Zurich, Zurich, Switzerland. [3]School of Science and Technology, IE University, Cardenal Zúñiga, Segovia, Spain. e-mail: lrosa@carnegiescience.edu

While solar PV presents a promising low-carbon energy solution for irrigation, a considerable challenge lies in the mismatch between renewable energy production and the timing of irrigation water demand. This temporal misalignment necessitates strategies for storing either water or electricity to ensure reliable operations. Despite the critical role of irrigation in global food production, few studies have applied macro energy system modeling and optimization to assess the alignment of renewable energy availability with irrigation water needs. Addressing this gap is essential to advance knowledge on achieving net-zero energy emissions in irrigation practices and optimizing renewable energy use for agricultural sustainability. Additionally, regional variations in irrigation water demands, irrigation systems, energy sources for pumping, and factors like groundwater depth create unique challenges. The impact of these regional differences on the cost-effectiveness or feasibility of net-zero emission solutions is not well understood.

Here, we design optimal irrigation systems to minimize both costs and energy-related $CO_2$ emissions, accounting for existing infrastructure and practices across 774 irrigated counties in the U.S., representing high irrigation demand areas and covering 98% of U.S. agricultural irrigation water use. A unique aspect of this work is the application of methodologies traditionally used in energy system modeling to water resources research. Specifically, we address the critical yet often-overlooked challenge of hourly mismatches between irrigation water demand and renewable energy availability, particularly from solar PV. We focus on solar PV systems as a distributed energy resource because they are cost-competitive, widely deployable at the farm scale, and can directly power irrigation infrastructure[24], while other options such as wind or hydropower face geographic, infrastructural, or scalability constraints in many agricultural regions[25,26]. Using a multi-objective analysis, for each county with irrigation in the U.S., we examine the trade-offs between cost and emissions for irrigation systems while incorporating detailed hourly modeling of energy production and water demand. This temporal granularity enables us to assess the alignment, or misalignment, between solar PV energy generation and irrigation water needs. To ensure water availability during periods of low or no solar PV production, we incorporate electricity and water storage solutions, such as batteries and water tanks. Our methodology accounts for regional variations in climate, agricultural practices, and energy resources. The U.S. was chosen for this analysis due to its important role as a global food producer, accounting for about 7% of the global harvested crop area[27], 13% of global cereal production by mass[27], and 6% of global agricultural irrigation water withdrawals[28]. Additionally, the U.S. offers comprehensive, reliable historical irrigation data at the county level, which is essential for this spatially explicit analysis[29].

By bridging energy system modeling with water research, our study provides a framework to explore pathways for achieving net-zero energy emissions in irrigation. This approach identifies energy-related cost-emission trade-offs while addressing challenges arising from location-specific water demands, renewable energy potential, and infrastructure constraints. This study aims to inform strategies for enhancing economic and environmental sustainability in agricultural water management, contributing to climate change mitigation and the resilience of agricultural systems.

## Results

### Optimization framework and scenario design

We developed a multi-objective optimization model using linear programming to minimize energy-related costs and $CO_2$ emissions (direct emissions from fuel combustion and indirect from electricity usage) from irrigated agriculture in the U.S. with a county level spatial resolution. The model determines the optimal portfolio of technologies, capacity expansion, and operations to minimize these objectives. Specifically, we quantified trade-offs associated with solar PV capacity, water storage, electricity storage via batteries, and the capacities and usage of electric and diesel water pumps.

To solve the model, we applied the epsilon constraint method[30], where energy-related costs are minimized while $CO_2$ emissions are incorporated as a constraint. By progressively reducing emission limits, the model identifies optimal solutions that balance costs and emissions. Based on these solutions, we define three key scenarios: (i) Business-as-Usual (BAU), (ii) Cost-Optimal, and (iii) Net-Zero, where energy-related emissions are fully eliminated. The BAU scenario reflects the continued operation of the currently installed diesel and electric pumps, without any new investments or technological changes. It represents the existing infrastructure and its associated operating costs, serving as a baseline for comparison, with the grid carbon intensity fixed at 2023 levels. The Cost-Optimal scenario aims to minimize total system costs without explicitly constraining $CO_2$ emissions. This scenario allows us to explore whether a purely cost-driven approach could lead to emissions reductions, thereby highlighting potential inefficiencies in the current irrigation system. Finally, the Net-Zero scenario imposes a constraint to eliminate both direct emissions from fuel combustion and indirect emissions from electricity use, representing a fully decarbonized irrigation system. The analysis accounts for energy and water balances, technology-specific constraints (e.g., maximum installed capacity, efficiency limits), and storage dynamics (e.g., charging or discharging losses). We optimized a single representative day of each month over the course of one year, reflecting the monthly resolution of water withdrawals data, while capturing the daily variation in water demand and solar PV energy production.

Figure 1 summarizes the methodological framework, which is described in detail in the Methods section. Input data (Fig. 1a), including irrigation types, water withdrawals, costs, $CO_2$ emissions, and technology parameters, undergo preprocessing (Fig. 1b) to ensure consistency and suitability for the optimization model. Preprocessing steps include calculating the energy required to pump water in each county based on groundwater depth and the shares of surface and groundwater, converting annual withdrawals to monthly, estimating the installed capacity of diesel and electric water pumps and aggregating hourly solar PV capacity factors into one representative day per month. The system design (Fig. 1c) integrates water pumps, solar PV, grid electricity, diesel, water storage, batteries, and irrigation technologies (drip, surface, and sprinkler). Figure 1d illustrates the model's spatial resolution at the county level and a temporal resolution of one representative day per month over a year. The optimization approach (Fig. 1e) is based on a multi-objective linear programming model that minimizes costs and $CO_2$ emissions using the epsilon constraint method. Finally, the outputs (Fig. 1f) outline possible transition pathways, including cost-optimal and net-zero emission solutions, as well as technology selection and operation strategies for irrigation systems.

### Trade-offs between cost and carbon emissions

Figure 2 presents the Pareto front between irrigation costs and energy-related emissions in the U.S. The curve spans the full design space, from net-zero emissions systems (achieved at higher costs) to today's high-emissions systems (associated with lower costs). This trade-off curve highlights how reducing emissions increasingly requires higher investment, while minimizing costs generally leads to higher emissions. The BAU scenario results in total costs of $3.8 billion per year and emits 9.89 Mt $CO_2$ emissions annually (Fig. 2) aligning with previous $CO_2$ emissions estimates[17]. We found that 33% of energy-related $CO_2$ emissions originate from diesel use, while the remaining 67% are attributed to grid electricity consumption annually (Fig. 2).

The cost-optimal scenario reduces both cost and $CO_2$ emissions compared to the BAU. It lowers total costs by $0.89 billion per year (−23%), bringing annual costs down to $2.95 billion per year (Fig. 2). Additionally, the cost-optimal scenario achieves a 39% (3.8 Mt $CO_2$ per year) reduction in $CO_2$ emissions, resulting in 6.1 Mt $CO_2$ per year (1.6%

https://doi.org/10.1038/s41467-026-71122-7

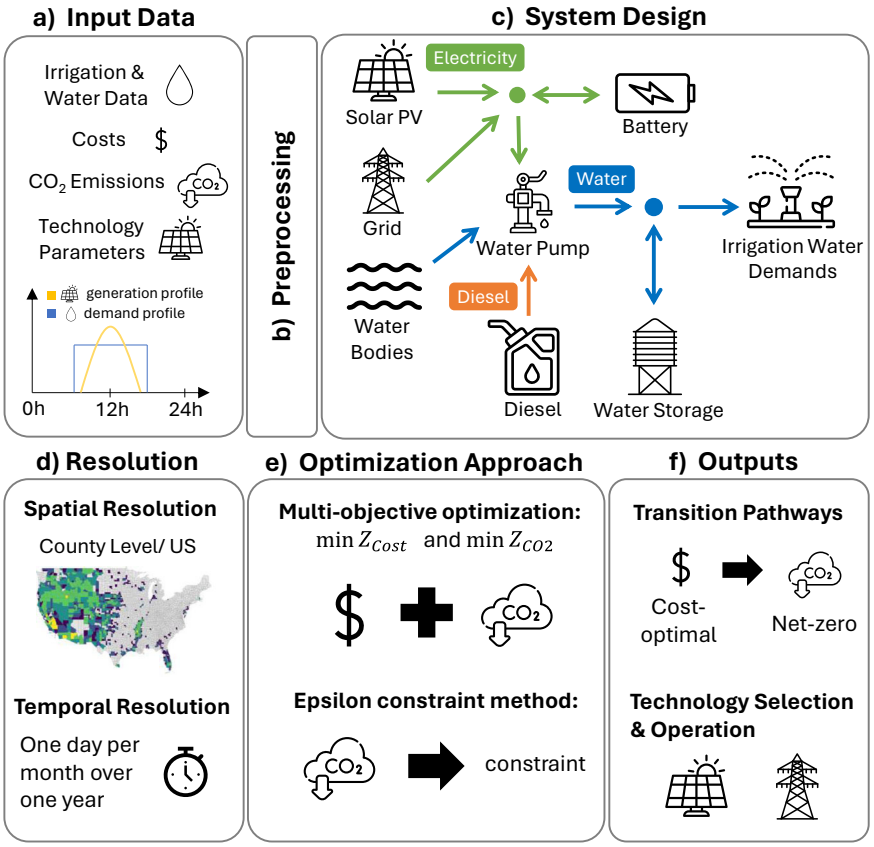


**Fig. 1 | Methodological framework for identifying optimal decarbonization pathways in irrigation systems based on energy-related costs and emissions.** **a** Input data include irrigation water demand, cost data, $CO_2$ emissions, and technology parameters. **b** Preprocessing converts raw input data into formats suitable for the optimization model. **c** The schematic illustrates the technologies (diesel and electric water pumps, water storage, batteries, solar photovoltaic (PV), and irrigation technology, drip, sprinkler, surface irrigation) and energy inputs (grid electricity, diesel, and solar PV) used in this analysis. Energy and water flows are color-coded: electricity in green, diesel in orange, and water in blue. **d** Spatial resolution focuses on county-level analysis across the U.S., while temporal resolution captures one representative day per month over a year. **e** Multi-objective optimization minimizes costs and $CO_2$ emissions using an epsilon constraint method. **f** Outputs provide transition pathways for cost-optimal and net-zero scenarios, detailing technology selection and operation. Icons from Flaticon or Microsoft PowerPoint. County boundaries from the U.S. Census Bureau 2023 Cartographic Boundary Files (data.gov).

from diesel and 98.4% from grid electricity) (Fig. 2). Further reductions in emissions can be achieved with minimal cost increase (Fig. 2). For instance, $CO_2$ emissions can be reduced to 1.53 Mt $CO_2$ per year, which is an 84.6% reduction compared to the BAU, with only exceeding the costs of the BAU scenario by 0.7% (Fig. 2). However, achieving net-zero emissions comes at a substantial cost, doubling total costs compared to the BAU scenario, reaching $8.0 billion per year (Fig. 2). The non-linear cost increase when approaching net-zero underscores the need to balance financial feasibility with environmental goals, particularly in addressing "last-mile" emission reductions.

In the BAU scenario, grid electricity accounts for 55.3% of total costs, while diesel contributes 27.5% (Fig. 2). In the cost-optimal scenario, diesel use is nearly eliminated (1.1%), the share of grid electricity falls slightly to 51.8%, and solar PV emerges as a major cost component, representing 21.5% of total costs. This shift indicates that solar PV-driven irrigation is a more cost-effective option than diesel pumping. In the net-zero scenario, the share of grid electricity drops to zero, as the grid is not carbon free. New cost contributions arise from solar PV (51.1%), battery storage (6.5%), and water storage (31.2%). Electric water pump costs remain essentially constant across all scenarios.

### Trade-offs in infrastructure deployment for $CO_2$ emissions reduction

Figure 3 illustrates the installed capacities of solar PV, water storage, batteries, and electric water pumps for varying levels of $CO_2$ emissions. These results underscore the complex trade-offs between achieving emissions reductions and the required infrastructure investments. As emissions approach net-zero, the cost increase becomes increasingly steep and non-linear, emphasizing the economic and operational challenges associated with stringent emission targets.

Grid electricity usage remains largely consistent between the BAU and cost-optimal scenarios (Fig. 3b) but is gradually reduced as emissions targets become more stringent, eventually being phased out completely in the net-zero scenario due to its associated emissions. Throughout this transition, electric pumps are increasingly supplied by renewable energy from newly installed solar PV systems (Fig. 3d). In contrast, diesel usage is already substantially lower in the cost-optimal scenario compared to BAU and continues to decline linearly as emissions reductions deepen, until they are fully eliminated in the net-zero scenario (Fig. 3a). This transition highlights key trade-offs. Diesel pumps are not cost-optimal due to their low efficiency (30% for diesel pumps vs. 80% for electric pumps). While grid electricity remains cost-effective for moderate decarbonization, net-zero scenarios require substantial investments in renewable energy, particularly solar PV.

Additional electric water pump capacity in the cost-optimal scenario reaches $1.13 \times 10^7$ $m^3$ $h^{-1}$ capacity compared to BAU, increasing gradually until emissions are reduced to 3.0 Mt $CO_2$ per year (Fig. 3c). Achieving net-zero emissions requires a 2.6-fold increase in capacity compared to the cost-optimal scenario. This oversizing reflects the need to maximize solar PV utilization, ensuring efficient use of

https://doi.org/10.1038/s41467-026-71122-7

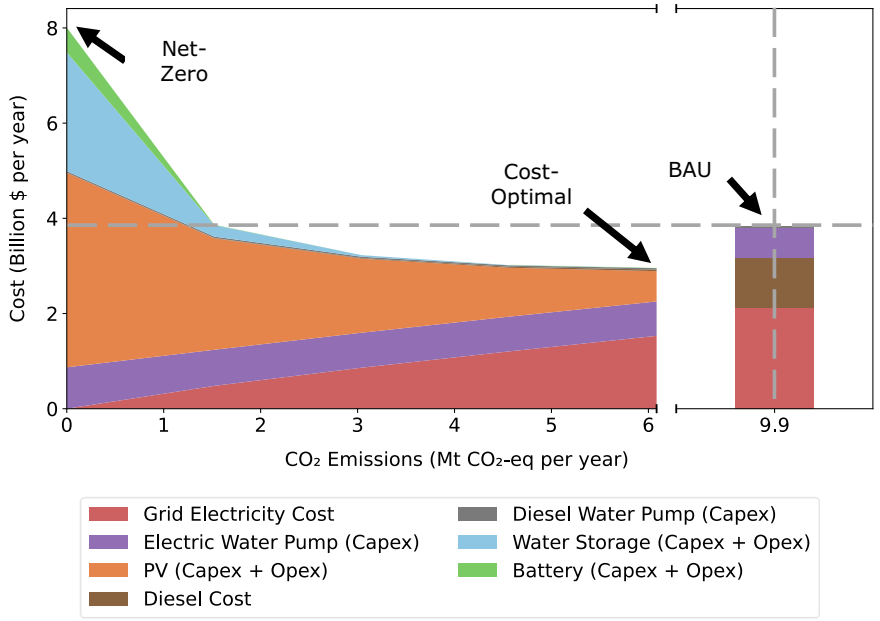


**Fig. 2 | Cost and carbon emissions trade-offs for irrigation transition pathways in the U.S.** The figure shows cost-emission trade-offs illustrated by a Pareto front, showing the optimization of total annual costs [billion $ per year] and $CO_2$ emissions [Mt per year], with cost contribution from each technology and energy feedstock. The graph compares the optimization results with the Business-as-Usual (BAU) scenario. Capex stands for "capital expenditure" while Opex is "operating expenditure".

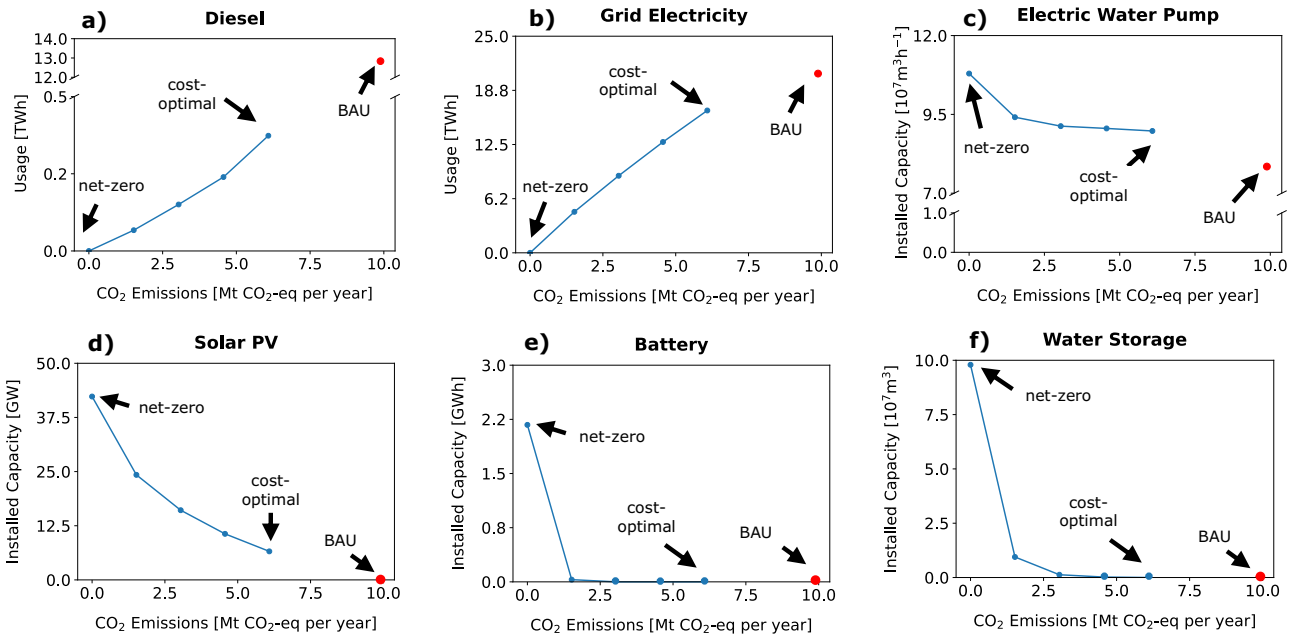


**Fig. 3 | Installed capacities of key technologies at varying $CO_2$ emission constraints.** Optimized tradeoffs between installed capacity and emissions (Pareto front) for different technologies across different levels of annual $CO_2$ emissions [Mt $CO_2$ per year]. **a** diesel usage [TWh], **b** grid electricity usage [TWh], **c** installed capacity of electric water pumps [$10^7$ $m^3h^{-1}$], **d** installed capacity of solar PV [GW], **e** installed energy storage capacity of batteries [GWh], **f** installed capacity of water storage [$10^7$ $m^3$]. The cost-optimal, net-zero, and business-as-usual (BAU) scenarios are highlighted for reference.

renewable energy during periods of high generation. However, this strategy introduces inefficiencies, as the oversized pump capacity may remain underutilized during periods of lower energy availability.

The steep increase in solar PV installations from 6.6 GW in the cost-optimal scenario to 42.3 GW in the net-zero scenario demonstrates the system's heavy reliance on solar energy to achieve emissions reductions (Fig. 3d). The U.S. had a total installed solar PV capacity of 122.1 GW in 2024[31], meaning that achieving net-zero irrigation in our scenario would require a capacity increase equivalent to almost 35% of the entire solar PV fleet. Given that solar PV installations require around 10 $km^2$ per GW[32], the cost-optimal scenario would necessitate between 66 $km^2$, while the net-zero scenario would require approximately 423 $km^2$. By comparison, California covers 424,000 $km^2$, and San Francisco County spans 121 $km^2$[33]. Expanding solar PV to this extent highlights the challenge of efficiently integrating growing generation into the system, raising concerns about resource use and overall efficiency. However, it also presents opportunities to repurpose curtailed energy for powering other industries or storing

energy for later use[34], which represents a relevant opportunity but is beyond the scope of this study.

Water storage capacity is not cost-effective at higher emissions levels but becomes essential as emissions approach net-zero. Storage is first deployed at an emission level of 1.5 Mt $CO_2$ per year, requiring $0.95 \times 10^7$ $m^3$ of capacity (Fig. 3f). At net-zero, the required water storage reaches $9.79 \times 10^7$ $m^3$, 1.64 times larger than California's Oroville Dam[35], the largest dam in the U.S., which holds ~$6 \times 10^7$ $m^3$. This large water storage requirements highlight a critical trade-off: as renewable energy dependence increases, so does the need for large-scale storage to buffer variability. This not only drives up costs but also intensifies resource consumption, including land, materials, and infrastructure, challenging the feasibility and sustainability of large-scale deployment.

Battery installations mirror the non-linear increase observed in water storage. While absent at higher $CO_2$ emissions levels, batteries become crucial as emissions approach net-zero, reaching a capacity of 2.2 GWh with an associated cost of $0.5 billion per year (Fig. 3e). For context, the U.S. planned 16 GW of utility-scale battery capacity by 2023; the battery storage required for net-zero in our scenario would represent 12.5% of this capacity[36]. The sharp increase reflects the need to store excess solar PV generation during peak periods and supply power during low-generation intervals.

### County-specific technology and energy sources

While Fig. 3 highlights the non-linear increase in installed capacities and fuel usage as emission constraints become stricter, Fig. 4 offers a spatial perspective on the deployment of energy sources (grid electricity and diesel) and technologies such as diesel water pumps, electric water pumps, solar PV, batteries, and water storage across U.S. counties. The spatial analysis reveals key trade-offs in the transition toward low-emission and net-zero systems, showing substantial heterogeneity across counties. This variability reflects differences in resource availability, infrastructure, and technological feasibility, shaping each county's pathway to decarbonization.

In the BAU scenario, no new capacity is added. Instead, existing diesel and electric water pump capacities are used to reflect current infrastructure as accurately as possible (Fig. 4a, d, g, j). Water pumping remains dependent on diesel and grid electricity, following present usage patterns. This scenario represents the status quo, illustrating how continued reliance on current systems leads to high operational costs and $CO_2$ emissions.

In the cost-optimal scenario, grid electricity and diesel usage decline substantially, particularly in counties with high energy conversion factors for water pumps (Fig. 4b, e). For example, Kansas and Oklahoma completely phase out diesel use due to its inefficiency. While diesel pump installations remain largely unchanged with minimal new deployments (Fig. 4k), electric water pump installations vastly increase in areas where diesel is more cost-intensive (Fig. 4h). Solar PV emerges as a dominant energy source across most regions, driven by its cost-competitiveness (Fig. 4n).

In the net-zero scenario, grid electricity and diesel are eliminated (Fig. 4c, f). The already existing diesel water pumps remain unused, and the missing capacity is replaced by electric water pumps (Fig. 4i, l). Solar PV becomes the sole energy source, with capacity expanding well beyond the cost-optimal scenario (Fig. 4o).

### County-specific costs

Figure 5 shows the annual irrigation costs per county and state, highlighting where investment is most critical to reduce energy-related carbon emissions. California has the highest contribution to total annual costs in the U.S., accounting for 21% under the BAU scenario, 18.7% under the cost-optimal scenario, and 15.1% under the net-zero scenario, due to its high irrigation water withdrawals of 24.9 $m^3$ (~17.0% of the national total)[17] and reliance on groundwater pumping. Following California are Arkansas (16.5% BAU scenario, 14.5% cost-optimal scenario, 18.7%), Nebraska (9.2% BAU scenario, 8.9% cost-optimal scenario, 9.5% net-zero scenario) and Idaho (8.5% BAU scenario, 10.6% cost-optimal scenario, 12.8% net-zero scenario).

Cost reduction in the cost-optimal scenario compared to BAU is driven by two main factors: the conversion efficiency of water pumps and the current distribution of diesel and electric pumps. Areas with high conversion factors for diesel pumps (Supplementary Fig. 1) also tend to have high conversion factors for electric pumps (Supplementary Fig. 2), as both are influenced by the relative shares of groundwater and surface water as well as groundwater depth, which are identical across the two technologies. Regions with high diesel pump usage benefit the most from switching to electric pumps, as the efficiency gains and cost savings are substantial. Conversely, regions with a high share of electric pumps are already closer to optimal efficiency, leaving less potential for further cost reductions. For example, Kansas and Oklahoma have very high conversion factors for water pumps and a large share of diesel pumps, leading to substantial cost-reduction potential. In contrast, some counties in Texas also exhibit high conversion factors for both pump types, but the state's low share of diesel water pumps limits its potential for cost reduction.

### Sensitivity analysis

A univariate sensitivity analysis was conducted to evaluate how variations in key parameters influence total costs and $CO_2$ emissions in the cost-optimal and net-zero scenarios. We varied cost parameters, efficiency factors of diesel and electric water pumps, and the annual emission factor of the electricity grid. The sensitivity analysis for cost parameters was performed by defining upper and lower bounds for the capital expenditures (capex) of all technologies, as well as for diesel and grid electricity prices (Supplementary Table 2). The sensitivity analysis (Fig. 6) shows that solar PV capital costs lead to the largest variation in model outputs. In the cost-optimal case, lowering PV capex by 4.0% reduces annual costs by 15% and $CO_2$ emissions by 43%. When PV capex is tripled (upper bound), costs rise by 11%, and emissions increase by 139%. This shows that the model output for emissions reacts more strongly to changes in PV capex than the output for costs, especially when PV becomes more expensive. In the net-zero case, PV capex variations affect costs between −25% and +46%.

Electric pump capex is the second most influential parameter after PV capex. In the cost-optimal scenario, electric pump capex changes annual costs by −16% to +69%, while the variation in emissions is comparatively small (−0.6% to +6.4%). The small change in emissions indicates that, even when electric pump capex is varied, the model does not shift substantially toward diesel pumping, which would otherwise lead to higher emissions. Electric pumping therefore, remains part of the cost-optimal technology mix across the tested range. Electric pump efficiency leads to cost variations of −8% to +5% and emissions variations of −11% to +7%. In the net-zero scenario, electric pump capex affects costs between −7% and +32%. Diesel-related parameters show limited effects. In the cost-optimal scenario, diesel pump capex leads to cost changes from −0.6% to +10% and no meaningful change in emissions, indicating that changes in diesel pump capex do not alter the technology choice in the model; if they did, emissions would vary. Diesel pump efficiency produces small variations in both costs (−1.3% to +0.4%) and emissions (−0.3% to +0.08%). Diesel fuel price leads to cost changes between −0.6% and +0.2% and emissions shifts between −2.3% and +1.8%. These results show that the outcomes presented in Fig. 3 are not sensitive to assumptions about diesel efficiency, diesel price, or diesel pump capex within the tested range.

Water storage capex has little influence in the cost-optimal scenario but affects costs by −12% to +24% in the net-zero scenario, reflecting the role of water storage in systems with high PV penetration. Battery capex produces minimal variation in both scenarios, with

https://doi.org/10.1038/s41467-026-71122-7

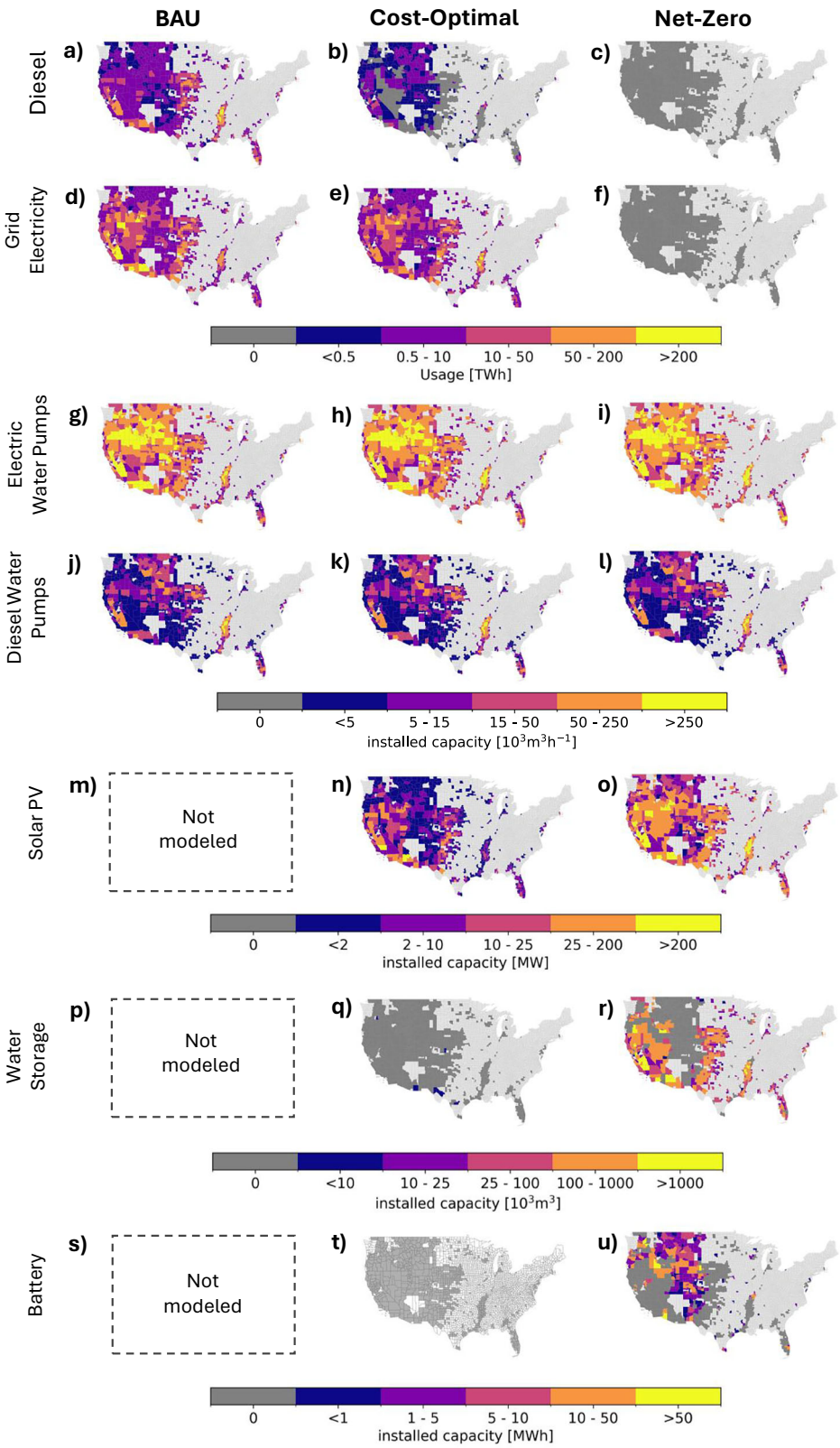


**Fig. 4 | Energy source usage and installed capacity per county for the Business-as-Usual, Cost-Optimal, and Net-Zero scenarios.** Energy source usage and installed capacity per county. Panels represent three scenarios: Business-as-Usual (BAU) (**a**, **d**, **g**, **j**, **m**, **p**, **s**), cost-optimal (**b**, **e**, **h**, **k**, **n**, **q**, **t**), and net-zero (**c**, **f**, **i**, **l**, **o**, **r**, **u**). Sub-figures show: diesel usage (**a**, **b**, **c**) [TWh], grid electricity usage (**d**, **e**, **f**) [TWh], installed capacity of electric water pumps (**g**, **h**, **i**) [$10^3$ $m^3$ $h^{-1}$], installed capacity of diesel water pumps (**j**, **k**, **l**)[$10^3$ $m^3h^{-1}$], installed capacity of solar PV (**m**, **n**, **o**) [MW], installed capacity of water storage (**p**, **q**, **r**) [$10^3$ $m^3$], and installed capacity of batteries (**s**, **t**, **u**) [MWh].

https://doi.org/10.1038/s41467-026-71122-7

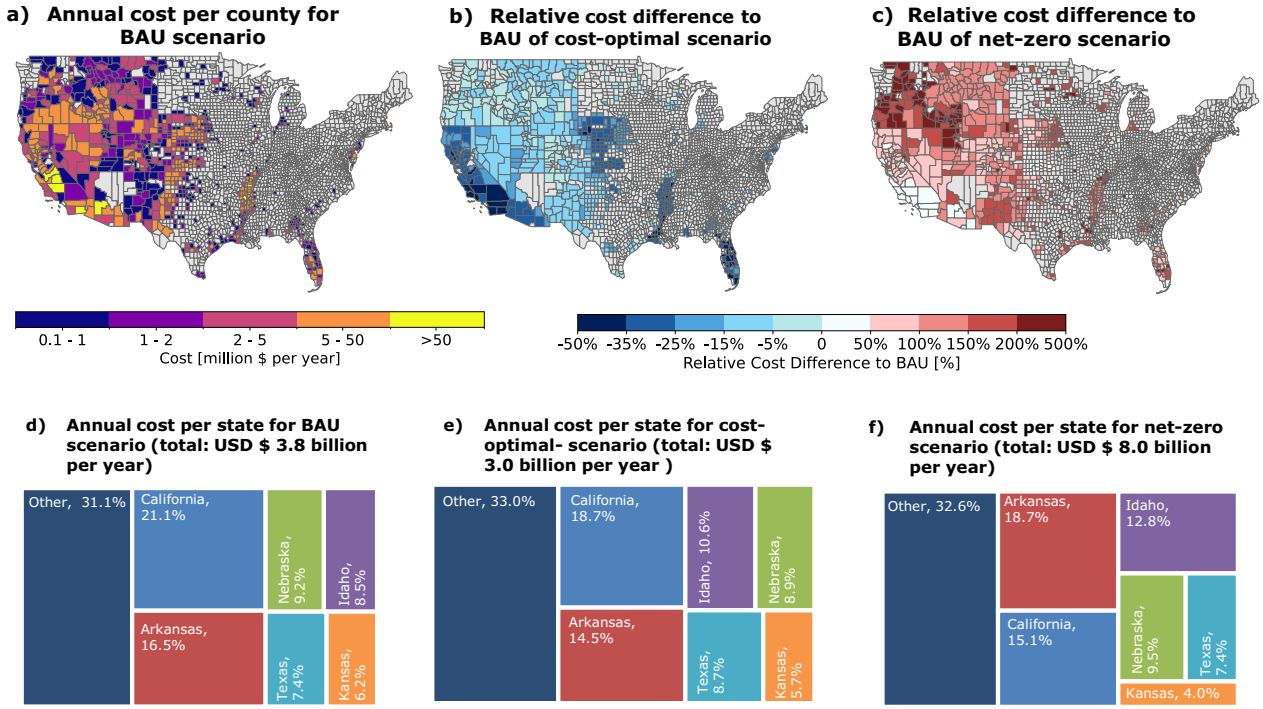


**Fig. 5 | Energy-related costs by county and state for Business-as-Usual (BAU), Cost-Optimal, and Net-Zero scenarios. a** Annual energy-related costs per county under the BAU scenario. **b** Relative cost differences compared to BAU per county under the cost-optimal scenario. **c** Relative cost differences compared to BAU per county under the net-zero-emissions scenario. **d** Total annual costs per state in the BAU scenario (total: $3.8 billion per year). **e** Total annual costs per state in the cost-optimal scenario (total: $3.0 billion per year). **f** Total annual costs per state in the net-zero-emissions scenario (total: $8.0 billion per year).

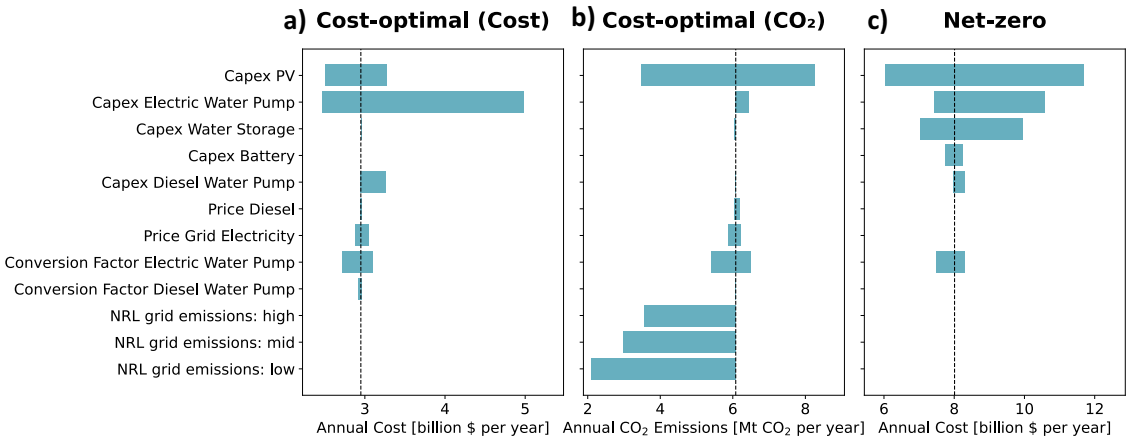


**Fig. 6 | Univariate sensitivity analysis.** This figure presents the results of a univariate uncertainty analysis, showing the impact of individual input variables on the upper and lower bounds of key output metrics, which can be found in Supplementary Table 1. **a** illustrates the variation in total annual costs for the cost-optimal scenario, **b** displays the variation in total annual $CO_2$ emissions for the cost-optimal scenario, and **c** shows the variation in total annual costs for the net-zero scenario. Each bar represents the range of possible outcomes resulting from changes in one input factor, such as the capital expenditures (Capex) for PV, electric water pumps, water storage, and batteries, diesel and grid electricity prices, efficiency for diesel and electric water pumps, and three National Laboratory of the Rockies long-run marginal emission rates[41] (mid-case (mid), high renewable energy cost (high), and 100% decarbonization by 2035(low)). The dashed line in each panel indicates the baseline output value.

changes below ±4%. Changes in grid electricity price leads to cost differences of −2.5% to +3.1% in the cost-optimal scenario, with emissions effects between −5.6% and +2.5%. Finally, variations in long-run marginal grid emission factors do not affect the net-zero scenario, as this scenario is independent of grid electricity given that the grid is not assumed to be fully decarbonized. The vertical line in Fig. 6 represents the baseline case based on 2023's grid emission intensity, while all three NRL sensitivity scenarios reflect future grid projections with lower carbon intensities. As a result, emissions in the cost-optimal scenario decrease (−41% to −66%), while technology choices and system costs remain unchanged, since only the grid emission factors vary.

## Discussion

Achieving a sustainable and resilient agricultural system requires cost-effectively decarbonizing energy-intensive irrigation. Our analysis reveals that the current irrigation system in the U.S. is highly inefficient in both costs and emissions (Fig. 2). The cost-optimal scenario demonstrates that more sustainable irrigation practices can also be

economically viable, simultaneously reducing costs and $CO_2$ emissions. Compared to BAU, this scenario lowers total costs by 23% ($0.89 billion per year) while achieving a 39% reduction in $CO_2$ emissions (3.8 Mt $CO_2$ per year) (Fig. 2).

The inefficiency of the BAU scenario primarily stems from its reliance on inefficient diesel water pumps and the absence of solar PV systems, which are critical for a low-carbon transition. Currently, only 0.7% of all water pumps in the U.S. are powered by solar energy, with 53% of these located in California[29]. This highlights a gap between cost-effective solutions and real-world implementation, likely due to limited technological awareness and insufficient financial support. While resources already exist to help farmers incorporate solar PV[37], the scale of funding and technical assistance may not yet fully meet demand.

A more ambitious 85% reduction in $CO_2$ emissions can be achieved with just a 0.7% increase in costs. However, achieving net-zero emissions requires substantial investments in solar PV, water storage, and batteries, ultimately doubling costs compared to the BAU scenario (Fig. 2). This non-linear cost increase underscores both the economic challenge and the importance of prioritizing large emission reductions as a first step, before pursuing complete elimination of emissions in a second stage. As reliance on renewables grows, oversized capacities and additional storage become necessary to counterbalance intermittency, introducing land and resource constraints that may vary locally. Solar PV expansion, for instance, reduces dependency on grid electricity and diesel but requires vast land and may create substantial land-use pressure, potentially competing with agricultural or conservation priorities[38], although successful examples of agrivoltaics demonstrate that co-existence is possible under certain conditions. Beyond these challenges, large-scale PV deployment also involves indirect emissions from manufacturing and installation that are not captured in our model. Future work incorporating a full life cycle assessment should discuss whether decarbonization efforts deliver a true net climate benefit. At the same time, the oversized PV capacities required for net-zero also present an opportunity: selling excess electricity back to the grid could provide additional revenue streams, partially offsetting system costs.

Although our results show that PV-powered pumping can be cost-optimal compared to diesel, real-world adoption remains limited due to several barriers. A key issue is the allocation of costs: diesel systems involve lower upfront cost but higher ongoing fuel expenses, while PV systems require a significant capital investment upfront but offer lower operating costs. Even when total costs over time are lower, farmers may lack the liquidity, credit access, or risk tolerance to invest in PV systems without appropriate financial support. Additional barriers include sunk costs in existing diesel equipment, uncertainty about performance, changes in farm routines, and limited familiarity with solar technologies. These factors help explain why PV systems are not yet widely deployed despite their modeled cost advantages. Closing this gap between modeled cost advantages and real-world deployment will require targeted financial instruments and improved access to technical support.

While these results highlight both the promise and complexity of large-scale irrigation decarbonization, the analysis is subject to several limitations that should be considered when interpreting the findings. Our study relies on historical data and therefore does not incorporate future changes in irrigation demand, or energy price. While this approach provides a clear baseline of the current system, integrating projections could offer a more dynamic view of future performance. A related limitation is that the model does not include the adoption of more efficient irrigation technologies, such as drip irrigation, as these are crop dependent and future irrigation expansion remain uncertain[12]. Transitioning to such systems often requires a change in crop type or is feasible only in specific regions, and farmers may be reluctant to adopt them given high upfront costs and familiarity with existing infrastructure.

Beyond scope decisions, several modeling choices were driven by computational tractability and data availability constraints. For instance, since water withdrawal data are only available at monthly resolution, we use one representative day per month. Although more advanced selection methods of representative day exist[39], the monthly data resolution prevents their application here. This approach still captures the main seasonal and monthly variability, but falls short in representing short-term fluctuations or prolonged drought events, which should be considered when interpreting results. A related simplification is the absence of hourly variation in grid $CO_2$ intensity, which may be relevant in regions with high solar penetration, where midday carbon intensity is significantly lower than evening peaks. Incorporating hourly grid emissions should be considered in future analysis. At the spatial level, county-level aggregation implicitly pools many individual farms into representative county assets, which may overestimate utilization and capacity factors of pumps and solar PV compared to site-specific operations. In practice, irrigation loads are small, non-coincident, and equipment is not freely shareable across fields, meaning discrete farm-scale units would likely have lower utilization and higher capex/opex than our aggregated estimates suggest. As high-resolution irrigated cropland datasets are becoming available, future analyses focused on specific regions could incorporate site-specific irrigation patterns, farm-scale equipment sizing, and utilization to provide more precise cost and capacity estimates.

Finally, the cost model itself has several important boundaries worth noting. Our analysis does not account for the additional capital required to extend electrical service to remote cropland, such as transmission lines, transformers, or service upgrades. This limitation has limited impact on the net-zero scenario, where solar systems can be deployed off-grid similarly to diesel setups. For groundwater-intensive regions transitioning to grid-connected electric pumps, these infrastructure costs could affect the overall cost assessment (Supplementary Note 1). Similarly, the model does not incorporate the age distribution of existing diesel and electric pumps, nor does it account for end-of-life value or phased replacement schedules. Since detailed infrastructure data are unavailable, sunk costs of existing equipment are not explicitly represented. As a result, the transition costs for individual farmers may differ from the system-level costs presented here, even though our results show that the annualized capex plus opex of new technologies is lower than the opex of continuing diesel operation. Finally, our comparison of diesel and electric pumps focuses on device-level efficiency, i.e., the energy required at the pump shaft per unit of diesel fuel or electricity consumed. We note that a full thermodynamic comparison would also include upstream conversion efficiencies of power generation and transmission losses. In our study, these upstream factors are already reflected in the emission intensity and cost of grid electricity, so they are not modeled separately. From the farmer's perspective, the relevant comparison is the cost and emissions of the fuels and electricity they purchase, rather than the primary energy inputs to the system.

Future work could advance this research along three directions. First, farm- and region-specific analyses incorporating site-specific irrigation schedules, crop-type constraints, and grid connection costs would improve cost and feasibility assessments, particularly in regions where electrification infrastructure remains underdeveloped. Second, optimizing on-farm electricity use, including the potential to sell excess solar generation back to the grid, could clarify the role of battery storage and reduce net system costs. Third, integrating projections of future irrigation demand, energy prices, and the evolving carbon intensity of the grid would enhance the long-term relevance of the model and better capture the interplay between agricultural decarbonization and broader energy transitions.

## Methods

### Energy requirements for irrigation water pumping

We assessed energy requirements for irrigation water pumping following the methods of Rosa et al.[14]. Irrigation energy requirement depends on the volume of water applied and the total pressure head, which is influenced by the type of irrigation system (drip, sprinkler, or surface), the energy source (diesel or electric), and the water source (surface or groundwater)[14,15].

To focus our analysis on areas with high irrigation demand, we selected counties where irrigation water demand exceeds the 75th percentile, resulting in a subset of 774 counties. While this includes only a fraction of all U.S. counties, these 774 counties account for 98% of the nation's total agricultural water demand. For each county, we calculated the energy required to pump water, considering variations in groundwater depth and irrigation system types. This is expressed using the conversion factor (CF), which quantifies the energy needed to pump a given water volume. Higher CF values indicate greater energy requirements for the same amount of water. Eq. 1 describes the computation of the CF for each county n ($CF_n$) following the calculation of Qin et al. [15]:

$$CF_n = \frac{EQ_n}{V_n} = \frac{TH_n}{367 \cdot \eta_{\text{pump}}} \tag{1}$$

$EQ_n$ denotes the energy input in kilowatt-hours (kWh), while $V_n$ is the volume of water being pumped in a county (n) in $m^3$. $TH_n$ represents the total water pressure head for each county expressed in meters (equivalent of the pressure of a 1-meter water column), and the pump's efficiency ($\eta_{\text{pump}}$) is 80% for electric water pumps and 30% for diesel pumps[21]. The factor 367 converts the total pressure head (in meters) to energy input (in kWh) for pumping 1 cubic meter of water, accounting for water density (1000 kg $m^{-3}$), gravitational acceleration (9.81 m $s^{-2}$), and unit conversion from joules to kWh.

The total pressure head ($TH_n$) for a given county $n$ (Eq. 2) consists of three components: the groundwater depth ($Lift_n$), the operating pressure ($H_n$), and the friction loss ($p_{\text{loss}}$), with the friction loss specified at 0.69 bar[15]. Groundwater depth is the vertical distance between the ground surface and the water table, indicating how far water must be lifted during pumping to reach the surface. Operating pressure depends on the water source and irrigation system type, expressed as the equivalent height of a water column. Friction loss refers to the energy lost as water moves through pipes, valves, and fittings due to resistance and turbulence in the flow. Since $p_{\text{loss}}$ is given in bars, it must be converted to meters using water density (ρ) and gravitational acceleration (g).

$$TH_n = \text{Lift}_n + H_n + \frac{p_{\text{loss}}}{\rho \cdot g} \tag{2}$$

The operating pressure ($H_n$) in meters for county n (Eq. 3) is calculated as the weighted sum of the pressures required for different irrigation system types and water sources. $b_{n,i}$ represents the share of each irrigation system[31] type i in county $n$, while $p_i$ denotes the pressure requirement (in bar) for irrigation system type. Here, i corresponds to the three irrigation system types: sprinkler, drip, surface. Similarly, $b_{n,gw}$[%] and $b_{n,sw}$[%] denote the shares of groundwater and surface water usage from Driscoll et al.[17] (Supplementary Fig. 3). The pressure requirements $p_i$ for each irrigation system using groundwater are 0.41 bar for surface irrigation, 1 bar for sprinkler systems, and 3 bar for drip irrigation[21]. The pressure associated with surface water bodies ($p_{sw}$) is 0 bar[15]. Since pressure is given in bars, it must be converted to meters to obtain the equivalent pressure head. This conversion is performed using water density (ρ) and gravitational acceleration (g), ensuring consistency with the total pressure head calculations.

$$H_n = \frac{1}{\rho \cdot g} \sum_{i \in I} b_{n,i} \cdot p_i \cdot b_{n,gw} + p_{sw} \cdot b_{n,sw} \tag{3}$$

The groundwater depth ($Lift_n$) (Eq. 4) is the weighted average of groundwater depth $d_n$[m], sourced by Lin et al. [40], adjusted by the share of groundwater use $b_{n,gw}$[%][17].

$$Lift_n = b_{n,gw} \cdot d_n \tag{4}$$

Because our analysis is at the county-level and detailed monthly data on groundwater depth are not available, energy losses due to groundwater decline are out of the scope of this study and are not quantified.

### Irrigation water withdrawals

Crop water demand is met either through rainfall ("green water") or irrigation ("blue water") when rainfall is insufficient[16]. Green water refers to moisture available in the plant's root zone, while irrigation water demand represents the supplemental water needed to meet crop needs[16]. Water withdrawal refers to the total volume of water extracted from natural sources (such as rivers, lakes, groundwater, and reservoirs) for irrigation purposes.

Monthly, county-level irrigation water withdrawals were derived by scaling annual irrigation water withdrawal data for 2015 from Driscoll et al. [17] with monthly distribution patterns provided by Huang et al. [41]. Driscoll's data builds upon the U.S. Department of Agriculture's dataset[2], resolving inconsistencies and providing a more detailed account of total water extraction for crop irrigation across U.S. counties. Huang's data were derived from four hydrological models (WaterGAP, H08, LPJmL, and PCR-GLOBWB for the years 2001 to 2010). These hydrological models provide monthly irrigation water data at a 5-arcminute resolution (approximately 10 km at the equator) for the period 2001–2010. For counties with missing monthly data in Huang et al.[41], state-level averages were used to fill the gaps. To assess the daily balance of energy and water flows, monthly irrigation water demand was converted to an hourly resolution. We assumed irrigation occurs evenly between 8 a.m. and 8 p.m., aligning with the daytime photosynthesis period when crops primarily require water. Monthly water demand was distributed across the number of days in each month and further divided by the 12-h irrigation window to calculate hourly demand.

### Solar PV

Hourly and county-specific solar PV capacity factors, representing the ratio of actual electricity generation to the maximum possible based on installed capacity, were sourced from Seel et al.[42] for the year 2022. These data, derived from the Lawrence Berkeley National Laboratory and based on historical irradiance estimates from NRL's National Solar Radiation Database, include values from multiple utility-scale solar projects[42]. When county-specific data were unavailable, state averages or data from Bracken et al.[43] were used as substitutes. To match the temporal resolution of water demand data, hourly solar PV capacity factors were averaged for each hour of a representative day in each month. This harmonization improved the analysis by ensuring both datasets aligned, enhancing the accuracy of the results. Details on capital costs[44], operational costs[44], and system lifetimes[45] can be found in Supplementary Table 3.

### Grid electricity and diesel prices

For diesel and grid electricity prices, we used state-level mean values from the years 2013 till 2023, with data from the U.S. Department of Agriculture[46] for diesel and the U.S. Energy Information Administration[47] for grid electricity. The carbon intensity of the grid

represents the grid of the year 2023[48]. The prices of diesel[46], grid electricity[47] and carbon intensity[48] of the grid are presented in Supplementary Figs. 4–6.

### Energy and water storage

Solar PV energy production does not always align with irrigation demand, making energy and water storage necessary. To address this, we considered batteries for energy storage and water tanks for water storage, as these are practical options for farmers. Capital and operational costs (battery[49], water storage[50,51]), lifespan (battery[50], water storage[52]), and charging and discharging efficiencies (battery[49]) were sourced from recent literature and are presented in Supplementary Table 3.

### Electric and diesel water pumps

In the BAU scenario, diesel and electric water pumps operate at the existing installed capacity (measured in $m^3\,h^{-1}$), without modeling any capacity expansion. Since no dataset reports installed water pump capacities, we estimated them by allocating each county's maximum hourly water demand to diesel and electric pumps based on the share of each energy source used. These shares were derived from state-level data on the number of electric and diesel pumps provided by the U.S. Department of Agriculture and applied uniformly to counties within each state[29] (Supplementary Fig. 7). The estimated capacities for each pump type, along with their capital costs[53,54] and lifetimes, are provided in Supplementary Table 3.

### Formulation of the optimization problem

We formulated and solved a linear programming optimization model that determines the cost, $CO_2$ emissions, installed capacities of technologies (electric and diesel water pumps, solar PV, batteries, water storage tanks) and the amount of used water, diesel, and grid electricity. The optimization problem was solved using Gurobi, a commercial solver[55]. We used the open-source model ZEN-Garden for running our simulation[56].

We conducted a one-year snapshot analysis for a representative future year, using current technology costs. Investment costs are annualized to equivalent annual cost using a 6% discount rate. The discount rate can be interpreted as either a social rate reflecting long-term societal welfare or a financial (investor) rate reflecting private capital costs and risk, with typical ranges of 3–5% and 6–12%, respectively[57]. Our use case lies between societal welfare and private capital perspectives, as it addresses long-term infrastructure planning while requiring implementation by individual farmers. We therefore applied a 6% discount rate, which reflects both perspectives and is commonly used in energy system studies[58]. To ensure that technologies are placed on a comparable economic basis we accounted for technology specific lifetimes while calculating the annualized investment costs. The BAU scenario reflects continued operation of the existing diesel and electric pump stock, while alternative scenarios allow investment in new technologies.

The multi-objective optimization problem aims to achieve two key objectives: minimizing cost and $CO_2$ emissions. To solve this problem, we employ the epsilon constraint method[30], where one objective is minimized while the other is converted into a constraint. The optimization problem is formulated for each county as Eq. 5:

$$\min_x Z_{cost} = q^T x \tag{5}$$

$$\text{subject to } Ax \le b, \tag{6}$$

$$x \in R^N$$

Where Z represents the objective function, in this case, the total system cost ($Z_{cost}$). The vector x contains the decision variables, q represents their coefficients, and they are combined into a linear function. The problem dimension, N, corresponds to the number of decision variables. The decision variables in our case are the amount of diesel and grid electricity [MW] used, as well as the capacity expansion of each technology (solar PV [MW], battery [MW], water storage [$m^3$], diesel and electric water pumps [$m^3h^{-1}$]). The inequality $Ax \le b$ (Eq. 6) defines the constraints in matrix form, where A is the constraint matrix, and b is a vector representing the upper limits of these constraints. These constraints ensure the solution satisfies the physical laws, or technical feasibility, such as energy balances, or capacity limitations. The full equation of all constraints can be found in the Supplementary Note 2.

Using the epsilon-constraint method (Eq. 7), $CO_2$ emissions were incorporated as a constraint within $Ax \le b$. First, the model is run without constraining $CO_2$ emissions, representing the unconstrained, cost-optimal scenario. This initial run determines the maximum $CO_2$ emissions ($f_{CO2,\,max}$) associated with the lowest-cost solution. Next, progressively stricter $CO_2$ emission constraints were applied, limiting emissions to 75%, 50%, 25%, and 0% of the cost-optimal value by setting α to 0.75, 0.50, 0.25, and 0, respectively (Eq. 7). Setting $CO_2$ emissions to 0% represents the net-zero energy emissions scenario.

$$Z_{CO2} \le \alpha \cdot f_{CO2,\,max},\ \alpha \in \{0.75,\ 0.5,\ 0.25,\ 0\} \tag{7}$$

The total system cost ($Z_{cost}$) include capital cost ($C_{capex}$) and operational cost ($C_{opex}$). The operational cost ($C_{opex}$) is adjusted by the discount factor (df) based on the interest rate (r) (Eq. 8). The discount factor is used to account for the time value of money, ensuring that costs incurred in different years are comparable by converting them to their present value (Eq. 9). This adjustment is necessary for accurately evaluating long-term investments and operational costs within the optimization framework.

$$Z_{cost} = C_{Capex} + C_{Opex} \cdot df \tag{8}$$

$$df = \frac{1}{1+r} \tag{9}$$

The capital cost ($C_{capex}$) (Eq. 10) is based on the installed capacity ($P_k$) and the annuity factor ($a_k$) (Eq. 11) of each technology k. Here, k denotes the set of technologies modeled, which includes electric water pumps, diesel water pumps, and the irrigation technology (drip, surface, and sprinkler).

The annuity factor ($a_k$) converts the upfront investment cost into an equivalent annual cost over the lifespan ($l_k$) of the technology, considering the interest rate (r).

$$C_{capex} = \sum_{k}^{K} C_{k,\,capex} \cdot P_k \cdot a_k \tag{10}$$

$$a_k = \frac{r}{1 - \frac{1}{(1+r)^{l_k}}} \tag{11}$$

The operational cost ($C_{opex}$) include operational cost of technologies ($C_{opex,techonology}$), costs associated with diesel ($C_D$) and electricity ($C_{El}$), as well as costs for $CO_2$ emissions ($C_{CO_2}$) (Eq. 12). The $CO_2$ emission cost is set to a nominal value of $0.05 per ton. This value is not intended to reflect real-world carbon prices or a social cost of carbon, but to act as a small penalty that avoids near cost-equivalent but high-emission solutions. We verified that this choice has no

material impact on results, as it contributes less than 1% to total costs.

$$C_{opex} = C_{opex,\,technology} + C_D + C_{El} + C_{CO_2} \tag{12}$$

The operational cost ($C_{opex,\,technology}$) is defined as the sum of three terms. The first term accounts for the variable operational costs ($C_{k,\,opexvariable}$) of each technology, multiplied by its usage ($U_{k,t}$) across all time steps (t). The second term represents the fixed operational costs per unit of power capacity ($C_{k,opex\ fixed\ power}$) multiplied by the installed power capacity ($P_{k,\,power}$). Finally, the third term accounts for the fixed operational costs per unit of energy capacity ($C_{k,\,opexfixedenergy}$) multiplied by the installed energy capacity ($P_{k,\,energy}$). Each of these terms is summed over all technologies (k) (Eq. 13). Supplementary Table 4 provides an overview of the units assigned to each variable and parameter in the operational cost equation for different technologies.

$$C_{opex,\,technology} = \sum_{t=1}^{T}\sum_{k}^{K} C_{k,\,opexvariable} \cdot U_{k,t} + \sum_{k}^{K} C_{k,\,opexfixedpower} \cdot P_{k,\,power} + \sum_{k}^{K} C_{k,\,opexfixedenergy} \cdot P_{k,\,energy} \tag{13}$$

The cost of diesel and electricity ($C_{El}$, $C_D$) is calculated as the product of the amount of diesel and electricity used ($U_{El}$, $U_D$) and their respective prices ($price_{El}$, $price_D$) (Eq. 14, Eq. 15).

$$C_{El} = \sum_{t=1}^{T} U_{El,t} \cdot price_{El} \tag{14}$$

$$C_D = \sum_{t=1}^{T} U_{D,t} \cdot price_D \tag{15}$$

The sources of $CO_2$ emissions are the energy feedstock, specifically diesel and grid electricity. This implies that minimizing $CO_2$ emissions involves reducing the amount of diesel and electricity ($U_{El}$, $U_D$) used. $CO_2$ emissions ($Z_{CO_2}$) are quantified as the product of the amount of diesel and electricity used ($U_{El}$, $U_D$) by their respective emission factor, $\gamma_{El}$,$\gamma_D$ (Eq. 16).

$$Z_{CO_2} = U_{El} \cdot \gamma_{El} + U_D \cdot \gamma_D \tag{16}$$

For emissions, we accounted for Scope 1 and 2 by including $CO_2$ emissions from energy sources such as diesel and grid electricity. Scope 1 refers to direct emissions from owned or controlled sources, while Scope 2 includes indirect emissions from the generation of purchased electricity, steam, heating, and cooling consumed by the reporting entity[59]. Scope 3 emissions, which cover all other indirect emissions across a company's value chain, were excluded from this analysis[59]. The carbon intensity of the grid is based on state-level 2023 data[48] and the carbon intensity of diesel was assumed to be 253.1 kg $CO_2$-eq per MWh[60].

### Sensitivity analysis

A univariate sensitivity analysis was conducted to evaluate how variations in key parameters influence total costs and $CO_2$ emissions in the cost-optimal and net-zero scenarios. We varied cost parameters, efficiency factors of diesel and electric water pumps, and the annual emission factor of the electricity grid. The sensitivity analysis for cost parameters was performed by defining upper and lower bounds for the capex of all technologies, as well as for diesel and grid electricity prices (Supplementary Table 2). The uncertainty range for solar PV system capex was obtained from the International Renewable Energy Agency[44]. To determine the range for diesel and electricity prices, we used data from the U.S. Department of Agriculture[46], and from the U.S. Energy Information Administration[47], respectively. These ranges represent the 5th and 95th percentiles of price data from the past decade. Battery cost ranges were sourced from Cole et al. [50]. For water storage, diesel water pumps, and electric water pumps, price data were collected from various online sources[51,53,54,61], and the 5th and 95th percentiles of these values were used to determine the bounds. A comprehensive table listing all references and parameter ranges can be found in Supplementary Table 2.

We assumed static efficiencies for electric and diesel pumps. In practice, pump efficiency depends on the installed pump types, flow rates, and pumping heads. Because detailed information on the pumps in use was not available, a flow-rate-based analysis was not feasible. Instead, we conducted a sensitivity analysis on pump efficiency using literature-based ranges: 15–50% for diesel pumps and 75–93% for electric pumps (lower bound: diesel and electric[62], lower bound: diesel[63] and electric[64]). From provided sources, we took the largest range available. All considered data sources are listed in the Supplementary Table 3. To account for different electricity grid conditions, we used long-run marginal emission rates provided by NRL[65], which capture changes in electricity demand, technology cost, fuel prices affect grid emissions[65] Annualized emission factors were calculated over a 20-year horizon using a 6% discount rate, consistent with the rest of the analysis. We evaluated three grid scenarios defined by NRL[65]: mid-case (mid), high renewable energy cost (high), and 100% decarbonization by 2035 (low), which together cover the highest expected variance in grid carbon emissions. The mid-case reflects moderate assumptions on technology costs, fuel prices, and demand growth under continuation of current policies, the high-cost scenario assumes higher renewable and battery costs, and the 100% decarbonization scenario represents an accelerated transition with rapid emissions reductions. In Supplementary Table 5 the annual grid emission values can be found for all NRL scenario as well as the annual value used for 2023 condition.

## Data availability

The data generated in this study have been deposited in the Zenodo database under accession code https://doi.org/10.5281/zenodo.18803044.

## Code availability

The code used in this study is available in the Zenodo repository at https://doi.org/10.5281/zenodo.18803044. The open-source ZEN-garden optimization framework is available at https://github.com/ZEN-universe/ZEN-garden.

## References

1. Beltran-Pea, A., Rosa, L. & D'Odorico, P. Global food self-sufficiency in the 21st century under sustainable intensification of agriculture. *Environ. Res. Lett.* **15**, 095004 (2020).
2. Zhang, X. et al. Quantitative assessment of agricultural sustainability reveals divergent priorities among nations. *One Earth* **4**, 1262–1277 (2021).
3. Rojas, M., Lambert, F., Ramirez-Villegas, J. & Challinor, A. J. Emergence of robust precipitation changes across crop production areas in the 21st century. *Proc. Natl. Acad. Sci. USA* **116**, 6673–6678 (2019).
4. Lesk, C. et al. Compound heat and moisture extreme impacts on global crop yields under climate change. *Nat. Rev. Earth Environ.* **3**, 872–889 (2022).
5. Rosa, L., Chiarelli, D. D., Rulli, M. C., Dell'Angelo, J. & D'Odorico, P. Global agricultural economic water scarcity. *Sci. Adv.* **6**, eaaz6031 (2020).
6. Rosa, L. & He, L. Global multi-model projections of green water scarcity risks in rainfed agriculture under 1.5 °C and 3 °C warming. *Agric. Water Manag.* **314**, 109519 (2025).

7. Rosa, L. Adapting agriculture to climate change via sustainable irrigation: biophysical potentials and feedbacks. *Environ. Res. Lett.* **17**, 063008 (2022).
8. Citrini, A., Sangiorgio, M. & Rosa, L. Global multi-model trends of unsustainable irrigation under climate change scenarios. *Environ. Res. Lett.* **20**, 104011 2025.
9. Rosa, L. et al. Closing the yield gap while ensuring water sustainability. *Environ. Res. Lett.* **13**, 104002 (2018).
10. Rosa, L., Chiarelli, D. D., Tu, C., Rulli, M. C. & D'odorico, P. Global unsustainable virtual water flows in agricultural trade. *Environ. Res. Lett.* **14**, 114001 (2019).
11. Scanlon, B. R. et al. Global water resources and the role of groundwater in a resilient water future. *Nat. Rev. Earth Environ.* **4**, 87–101 (2023).
12. Rosa, L. et al. Potential for sustainable irrigation expansion in a 3 °C warmer climate. *Proc. Natl. Acad. Sci. USA* **117**, 29526–29534 (2020).
13. Rosa, L. & Sangiorgio, M. Global water gaps under future warming levels. *Nat. Commun.* **16**, 1192 (2025).
14. Rosa, L. et al. Energy implications of the 21st century agrarian transition. *Nat. Commun.* **12**,2319 (2021).
15. Qin, J. et al. Global energy use and carbon emissions from irrigated agriculture. *Nat. Commun.* **15**, 3084 (2024).
16. Ren, C. & Rosa, L. Global energy and carbon emissions of irrigation and fertilizers management for closing crop yield gaps. *Environ. Res. Lett.* **20**, 104026 (2025).
17. Driscoll, A. W., Conant, R. T., Marston, L. T., Choi, E. & Mueller, N. D. Greenhouse gas emissions from US irrigation pumping and implications for climate-smart irrigation policy. *Nat. Commun.* **15**, 675 (2024).
18. Driscoll, A. W. et al. Hotspots of irrigation-related US greenhouse gas emissions from multiple sources. *Nat. Water* **2**, 837–847 (2024).
19. Anand, S. K., Rosa, L., Mohanty, B. P., Rajan, N. & Calabrese, S. Balancing productivity and climate impact: a framework to assess climate-smart irrigation. *Earths Future* **13**, e2025EF006116 (2025).
20. Qian, H. et al. Greenhouse gas emissions and mitigation in rice agriculture. *Nat. Rev. Earth Environ.* **4**, 716–732 (2023).
21. McCarthy, B. et al. Trends in water use, energy consumption, and carbon emissions from irrigation: role of shifting technologies and energy sources. *Environ. Sci. Technol.* **54**, 15329–15337 (2020).
22. Rosa, L. & Gabrielli, P. Achieving net-zero emissions in agriculture: a review. *Environ. Res. Lett.* **18**, 063002 (2023).
23. Barron-Gafford, G. A. et al. Agrivoltaics provide mutual benefits across the food–energy–water nexus in drylands. *Nat. Sustain.* **2**, 848–855 (2019).
24. Pandey, G., Lyden, S., Franklin, E., Millar, B. & Harrison, M. T. A systematic review of agrivoltaics: productivity, profitability, and environmental co-benefits. *Sustain Prod. Consum* **56**, 13–36 (2025).
25. McKenna, R. et al. System impacts of wind energy developments: Key research challenges and opportunities. *Joule* **9**, 101799 (2025).
26. Moran, E. F., Lopez, M. C., Moore, N., Müller, N. & Hyndman, D. W. Sustainable hydropower in the 21st century. *Proc. Natl. Acad. Sci. USA* **115**, 11891–11898 (2018).
27. Food and Agriculture Organization of the United Nations. FAOSTAT: Food and Agriculture Organization Corporate Statistical Database. https://www.fao.org/faostat/en/#data (accessed November 2024).
28. Food and Agriculture Organization of the United Nations. AQUASTAT: Global Information System on Water and Agriculture. https://data.apps.fao.org/aquastat/?lang=en (accessed November 2024).
29. National Agricultural Statistics Service. *2018 Irrigation and Water Management Survey*. United States Department of Agriculture, Washington DC. https://www.nass.usda.gov/Publications/AgCensus/2017/Online_Resources/Farm_and_Ranch_Irrigation_Survey/index.php (2019).
30. Mavrotas, G. Effective implementation of the ε-constraint method in multi-objective mathematical programming problems. *Appl. Math. Comput.* **213**, 455–465 (2009).
31. U.S. Energy Information Administration. Table 4.7.B. Net Summer Capacity Using Primarily Renewable Energy Sources and by State, 2024 and 2023 (Megawatts). *Electric Power Annual*. https://www.eia.gov/electricity/annual/html/epa_04_07_b.html (accessed October 2025).
32. Bolinger, M. & Bolinger, G. Land requirements for utility-scale PV: An empirical update on power and energy density. *IEEE J. Photovolt.* **12**, 589–594 (2022).
33. U.S. Census Bureau. San Francisco County California. https://data.census.gov/. (accessed January 2024).
34. Ganter, A., Ruggles, T. H., Gabrielli, P., Sansavini, G. & Caldeira, K. Utilizing curtailed wind and solar power to scale up electrolytic hydrogen production in Europe. *Environ. Sci. Technol.* **59**, 3495–3507 (2025).
35. . Wikipedia. Oroville Dam. https://en.wikipedia.org/w/index.php?title=Oroville_Dam&oldid=1234513773. (accessed August 2024).
36. Antonio, K. & Mey, A. U. S. battery storage capacity expected to nearly double in 2024. *U.S. Energy Information Administration* https://www.eia.gov/todayinenergy/detail.php?id=61202 (accessed January 2025).
37. Office of Energy Efficiency and Renewable Energy. Farmer's Guide to Going Solar. https://www.energy.gov/eere/solar/farmers-guide-going-solar. (accessed August 2024).
38. Gabrielli, P., Goericke, H. & Rosa, L. Optimal combination of net-zero pathways for minimum energy, land, and water consumption in chemical production. *Ind. Eng. Chem. Res.* **63**, 13929–13942 (2024).
39. Gao, S. et al. Spectral clustering-based demand-oriented representative days selection method for power system expansion planning. *Int. J. Electr. Power Energy Syst.* **125**, 106560 (2021).
40. Lin, C. Y., Miller, A., Waqar, M. & Marston, L. T. A database of groundwater wells in the United States. *Sci. Data* **11**, 335 (2024).
41. Huang, Z. et al. Reconstruction of global gridded monthly sectoral water withdrawals for 1971-2010 and analysis of their spatiotemporal patterns. *Hydrol. Earth Syst. Sci.* **22**, 2117–2133 (2018).
42. Seel, J., Mills, A., Millstein, D., Gorman, W. & Jeong, S. Solar-to-Grid Public Data File for Utility-scale (UPV) and Distributed Photovoltaics (DPV) Generation, Capacity Credit, and Value. *Open Energy Data Initiative (OEDI)*, Lawrence Berkeley National Laboratory. https://doi.org/10.25984/1787566 (2020).
43. Bracken, C., Underwood, S., Campbell, A., Thurber, T. B. & Voisin, N. Hourly wind and solar generation profiles for every EIA 2020 plant in the CONUS. *Zenodo* https://doi.org/10.5281/zenodo.7901615 (2023).
44. International Renewable Energy Agency. *Renewable Power Generation Costs in 2022*. IRENA, Abu Dhabi https://www.irena.org/Publications/2024/Sep/Renewable-Power-Generation-Costs-in-2023 (2023).
45. Sodhi, M., Banaszek, L., Magee, C. & Rivero-Hudec, M. Economic Lifetimes of Solar Panels. *Procedia CIRP* **105**, 782–787 (2022).
46. United States Department of Agriculture. Historical Diesel Fuel Prices. https://agtransport.usda.gov/Fuel/Historical-Diesel-Fuel-Prices/u2kh-s8ke (accessed July 2024).
47. U.S. Energy Information Administration. State Electricity Profiles: 2013 to 2023. https://www.eia.gov/electricity/. (accessed November 2024).
48. Carnegie Mellon University. Power Sector Carbon Index. https://www.emissionsindex.org (accessed January 2025).
49. Mongird, K. et al. *2020 Grid Energy Storage Technology Cost and Performance Assessment*. Technical Report DOE/PA-0204, U.S. Department of Energy, Washington DC https://www.pnnl.gov/

sites/default/files/media/file/Final%20-%20ESGC%20Cost%20Performance%20Report%2012-11-2020.pdf (2020).
50. Cole, W., Frazier, A. W. & Augustine, C. *Cost Projections for Utility-Scale Battery Storage: 2021 Update*. Technical Report NREL/TP-6A20-79236, National Renewable Energy Laboratory, Golden, CO https://docs.nrel.gov/docs/fy21osti/79236.pdf (2021).
51. Tank Depot. Water Tanks. https://www.tank-depot.com/ (accessed July 2024).
52. Smart Water Technology. How long will my water tank last? https://smartwateronline.com/news/how-long-will-my-water-tank-last (accessed January 2025).
53. Absolute Water Pumps. Absolute Water Pumps - Water Pumps & Accessories. https://www.absolutewaterpumps.com/ (accessed July 2024).
54. Pump Stop Online. Agriculture Water Pump. https://pumpstoponline.com/ (accessed July 2024).
55. Gurobi Optimization LLC. Gurobi Optimizer Reference Manual. https://www.gurobi.com (2024).
56. Mannhardt, J. et al. ZEN-garden: Optimizing energy transition pathways with user-oriented data handling. *SoftwareX* **29**, 102059 (2025).
57. García-Gusano, D., Espegren, K., Lind, A. & Kirkengen, M. The role of the discount rates in energy systems optimisation models. *Renew. Sustain. Energy Rev.* **59**, 56–72 (2016).
58. Ganter, A., Gabrielli, P. & Sansavini, G. Near-term infrastructure rollout and investment strategies for net-zero hydrogen supply chains. *Renew. Sustain. Energy Rev.* **194**, 114314 (2024).
59. U.S. Environmental Protection Agency. Greenhouse Gas Reporting Program (GHGRP). https://www.epa.gov/ghgreporting (accessed July 2024).
60. U.S. Energy Information Administration. Carbon Dioxide Emissions Coefficients. https://www.eia.gov/environment/emissions/co2_vol_mass.php (accessed April 2024).
61. Rainwater Equipment, 2024. Rainwater Equipment. https://rainwaterequipment.com/. (accessed July 2024).
62. Stringam, B. Pump Efficiency. LSU AgCenter Publication 3241-J, Louisiana State University Agricultural Center, Baton Rouge, LA https://www.lsuagcenter.com/portals/communications/publications/publications_catalog/environment/irrigation/irrigation_pumping_plant_efficiency_testing_series/pump-efficiency (2013).
63. Harrison, K. A. Irrigation Pumping Plants and Energy Use. University of Georgia Cooperative Extension Bulletin B 837, University of Georgia, Athens, GA https://fieldreport.caes.uga.edu/publications/B837/irrigation-pumping-plants-and-energy-use/ (2011).
64. Evans, R., Sneed, R. E. & Hunt, J. H. Pumping Plant Performance. NC State Extension Publication AG-452-6, North Carolina State University, Raleigh, NC https://drainage.wordpress.ncsu.edu/files/2017/04/ag-452-6-pumping-plant-evans.pdf (1996, revised 2024).
65. Gagnon, P. Long-run marginal emission rates for electricity - workbooks for 2023 Cambium Data. *NLR Data Catalog*, National Laboratory of the Rockies, Golden, CO. https://doi.org/10.7799/2305481 (2024).

## Acknowledgements

J.S. thanks Johannes Burger and the Reliability and Risk Engineering Lab at ETH Zurich for advice on using ZEN-Garden.

## Author contributions

L.R. conceived and supervised the research. J.S. developed the model, performed the simulations, and analyzed the data. J.S., S.M., and L.R. designed the study, interpreted the results, and contributed to writing the manuscript.

## Competing interests

The authors declare no competing interests.

## Additional information

**Supplementary information** The online version contains supplementary material available at https://doi.org/10.1038/s41467-026-71122-7.

**Correspondence** and requests for materials should be addressed to Lorenzo Rosa.

**Peer review information** *Nature Communications* thanks Pratham Arora, Stuart Cohen and the other anonymous, reviewer(s) for their contribution to the peer review of this work. A peer review file is available.